Research Article
DOI: http://dx.doi.org/10.2110/palo.2017.051
EXPERIMENTAL TAPHONOMY OF KERATIN: A STRUCTURAL ANALYSIS OF EARLY TAPHONOMIC CHANGES
EVAN T. SAITTA,[1] CHRISTOPHER S. ROGERS,[2] RICHARD A. BROOKER,[1] AND JAKOB VINTHER[1,3]
[1]School of Earth Sciences, University of Bristol, Wills Memorial Building, Queens Road, Bristol, BS8 1RJ, UK
[2]School of Biological, Earth and Environmental Sciences, University College Cork, Distillery Field, N Mall, Cork, T23 XA50, Ireland
[3]School of Biological Sciences, University of Bristol, Life Sciences Building, Tyndall Avenue, Bristol, BS8 1TQ, UK
email: evansaitta@gmail.com
ABSTRACT: The evolution of integumentary structures, particularly in relation to feathers in dinosaurs, has become an area of intense research. Our understanding of the molecular evolution of keratin protein is greatly restricted by the fact that such information is lost during diagenesis and cannot be derived from fossils. In this study, decay and maturation experiments are used to determine if different keratin types or integumentary structures show different patterns of degradation early in their taphonomic histories and if such simulations might advance our understanding of different fossilization pathways. Although different distortion patterns were observed in different filamentous structures during moderate maturation and ultrastructural textures unique to certain types of scales persisted in moderate maturation, neither of these have been observed in fossils. It remains uncertain whether these degradation patterns would ever occur in natural sediment matrix, where microbial and chemical decay happens well before significant diagenesis. It takes some time for remains to be buried, meaning that keratin may not be left for moderate maturation to produce such patterns. Higher, more realistic maturation conditions produce a thick, and water soluble fluid that lacks all morphological and ultrastructural details of the original keratin, suggesting that such textural or distortion patterns are unlikely to be preserved in fossils. Although different degradation patterns among keratinous structures are intriguing, it is unlikely that such information could be recorded in the fossil record. Calcium phosphates and pigments are the surviving components of integumentary structures. Thus, the results here are likely of more relation to the archaeological record than fossil record. Other noteworthy results of these experiments are that melanin may not be the leading factor in determining the rate of microbial decay in feathers but may reduce the rate of degradation from maturation, that the existence of rachis filamentous subunits similar to plumulaceous barbules is supported, and that previously reported dinosaur 'erythrocytes' may be taphonomic artifacts of degraded organic material.
INTRODUCTION
Keratins such as feathers, pelts, and hair, spun and weaved into textiles, are rare in archaeological sites (e.g., Hargrave 1960; Messinger 1965; Brom 1986; Reinhard and Bryant 1992; Rogers et al. 2002; Dove et al. 2005). Although peptides can persist in some circumstances due to anaerobic, acidic conditions and occasionally through the association with toxic metals (e.g., copper), iron presence results in only a corrosion cast and/or pseudomorphs of the keratin (Solazzo et al. 2014; O'Connor et al. 2015). Millennia of diagenetic forces can degrade keratin,

which is robust relative to other proteins due to extensive disulphide cross-linking by the amino acid, cysteine.

Avian and 'reptilian' scales are essentially folded epidermis and possess a thin, flexible layer called the hinge region and a hard, thick, corneous outer surface (Wyld and Brush 1979, 1983; Sawyer et al. 2000). Feathers are tubular, and often fractal, integumentary structures originating from a feather follicle (Prum and Brush 2002). In recent years, many non-avian dinosaur fossils have been found with preserved feathers, making the topic of feather evolution a popular and important area of research for understanding the origin of bird flight, visual communication, and endothermy (see Xu and Guo 2009 for a review). The presence of extinct feather morphologies (e.g., Zhang et al. 2008) beyond those expected from an evo-devo approach (Prum and Brush 2002) and the discovery of feather-like integumentary appendages in a number of ornithischian dinosaurs, some of which may not represent 'true feathers' (Godefroit et al. 2014; Mayr et al. 2016), add complexity to feather evolutionary history.

Feathers, like all integumentary appendages, consist of keratin protein. Keratins are a common and highly diverse group of fibrous structural proteins (Fraser et al. 1972). While mammalian hair consists of α-keratin (Hill et al. 2010), 'reptiles' and birds are the only group to possess β-keratin (Prum and Brush 2002). β-keratin is itself diverse. 'Reptilian' scales, along with the reticulate scales of birds, consist of non-featherlike β-keratin on the outer surface in addition to α-keratin in the hinge region (Wyld and Brush 1979, 1983; Prum and Brush 2002). Birds in particular possess a more derived group of β-keratins known as ϕ-keratin (Brush 1978), now believed to be distributed more widely in archosaurs than originally thought. Avian scutate scales, claws, and beaks consist of a more basal ϕ-keratin than the ϕ-keratin of feathers, and scutate scales potentially evolved via modification of leg feathers (Prum and Brush 2002). One interesting implication of this hypothesis is that it opens up the possibility that certain extinct scaly taxa or taxa partially covered in scales might represent secondarily featherless forms. The keratin of crocodilian claws is highly related to the ϕ-keratins in avian scutate scales, beaks, and claws, making ϕ-keratins widely distributed in archosaurs (Sawyer et al. 2000). This ϕ-keratin has also been observed in embryonic alligator scales, although the scales of older individuals consist of typical 'reptilian', non-featherlike β-keratin, or in others word, not ϕ-keratin (Alibardi et al. 2005). Interestingly, the bristles of the turkey beard are not considered to be 'true' feathers in their structure and development (Schorger 1957), and consist of both feather-type and avian scutate scale-type ϕ-keratin (Sawyer et al. 2003). Thus, ϕ-keratins possibly appeared in an Archosaurian ancestor to birds and crocodilians and then diversified. Molecular phylogenies suggest scutate scale ϕ-keratin genes form a monophyletic basal-most group. In turn, claw ϕ-keratin genes form a monophyletic group basal to all feather ϕ-keratin genes. Integument evolution involved a duplication and divergence of ancestral β-keratin gene clusters. This gene family expanded alongside morphological diversification of integumentary appendages (Greenwold and Sawyer 2010). Molecular dating predicts that basal ϕ-keratin diverged ~ 216 Ma and feather ϕ-keratins diverged ~ 143 Ma, younger than the oldest feathered dinosaurs. If correct (it is unconstrained by fossil data), then early feathers may not have been made out of modern feather-specific ϕ-keratin. The appearance of feather ϕ-keratin after the evolution of feathers might have impacted biomechanical performance during powered flight (Greenwold and Sawyer 2011). Thus, if taphonomy can provide insight into the molecular evolution of keratin, the implications for paleobiological analyses of extinct taxa could be far-reaching.

Here we investigate whether or not different keratin types or keratinous structures show varied morphological and ultrastructural degradation patterns early in their taphonomic history. Although keratin protein is not likely to ultimately survive in Mesozoic fossils (see Briggs and Summons 2014; Saitta et al. 2017, contra Moyer et al. 2016; Pan et al. 2016), might variation in early taphonomic patterns be detectable in fossils? If so, fossils would be able to provide information about the molecular evolution of keratinous structures in addition to their morphological evolution.

METHODS

Fresh Samples

Samples were gathered from a range of extant integumentary structures, including feathers, scales ('reptilian' and avian), avian bristles, and mammalian hair (Table 1).

This study focused on white, black, and iridescent feathers. Feathers were collected from a deceased male bronze turkey (*Meleagris gallopavo*) and male light Sussex chicken (*Gallus gallus*) ordered from UK farms. Feathers were plucked from the body and sorted according to body region (back, belly, neck, wing coverts, primaries, secondaries, tail, legs) and stored in a laboratory freezer to prevent any decay until experimentation. The light Sussex chicken was selected for its black and white plumage, acting as a control when examining taphonomic differences between pigmented and non-pigmented feathers. It is mostly white, but has black feathers on the wings and tail. Many feathers on the neck are black with a white fringe. The feathers from the turkey are heavily pigmented and some are iridescent. The bristles of the turkey beard, along with the epidermal outgrowth that supports the bristles, were dissected and placed in the freezer. However, the male bronze turkey provided was younger than expected—it only had very short bristles. To supplement this, dried beards of wild turkeys (same species as the domestic turkey) from older individuals with longer bristles were supplied from a US hide and fur business. Although their dried nature might change degradation processes in these samples, they allowed for characterization of beard taphonomy according to ontogeny, which is important due to the unusual developmental patterns of beards (Schorger 1957). Dried beards were not placed in the freezer, as this was deemed unnecessary given the time between sourcing and experimentation. Drying a tissue prior to maturation would be expected to slow the rate of peptide hydrolysis, although air moisture trapped within maturation capsules may very well counteract this and make the difference between fresh and dried bristles moot. Regardless, any differences in degradation patterns found between the fresh and dried bristles, although interesting given the ontogeny of turkey beards, should be more carefully tested in future work.

Legs from the turkey were removed and placed in the freezer. Scutate and reticulate scales were later obtained from the legs via dissection.

Pigmented and non-pigmented scales were obtained from the flank of a large, male Nile crocodile (*Crocodylus niloticus*). No single scale is a solid color, so the designation refers to the predominant level of pigmentation across the scale. The skin sample was provided by La Ferme Aux Crocodiles (Pierrelatte, France). Scales were stored in the freezer.

The mane of a domestic horse (*Equus ferus*) was obtained from the Equine Centre of Langford Veterinary Services (Bristol, UK). This sample was also not placed in the freezer as experimentation occurred shortly after acquisition.

Decayed Samples

Naturally occurring turkey feather microbes were cultured in a sterile (autoclaved) flask according to the methods presented in Williams et al. (1990) using one liter of salt broth of the following composition (in grams/liter): 0.5 NH_4CL; 0.5 NaCl; 0.3 K_2HPO_4; 0.4 KH_2PO_4; 0.1

$MgCl\text{-}6H_2O$; 0.1 yeast extract. Microbes were introduced by placing darkly pigmented turkey belly feathers in the salt broth. This microbial broth was incubated for 56 days at ~ 37.5°C at 150–200 rpm. After one day of incubation, the broth had become murky, and clear signs of decay were present after one month of incubation. Many small bits of feathers separated and floated in the broth, indicating protein degradation. However, most of the feathers still retained much of their original form.

Black, white, and iridescent feathers (Table 1) were placed in separate Pyrex jars according to feather color. Clean salt broth was then poured into the jars with a small amount of the cultured microbial broth added to introduce the microorganisms needed for rapid decay. During pouring, the cultured microbial broth was filtered through a fine nylon mesh to prevent the previous feathers from contaminating the experimental samples. Plastic spacers were used to keep the feathers submerged. As a control, another jar contained four darkly pigmented turkey back feathers in mineral water. The four jars were incubated at ~ 37°C for 50 days (a power outage likely caused temperatures to drop for several days during this time but would have affected all decayed samples in the study equally as all sample jars were decayed simultaneously in the same oven). At the end of the decay process, decayed feathers were removed from the Pyrex jars with tweezers or filtered out with a fine nylon mesh depending on their level of degradation and then rinsed with ethanol on top of filter paper to clean them and prevent further decay.

Maturation

Subsets of the fresh and decayed samples were subjected to maturation through autoclaving using a cold-seal pressure vessel (University of Bristol), see Table 1 as well as Online Supplemental material for details about quantities of samples matured. Samples were decontaminated by rinsing in acetone prior to loading into $Au_{90}Pd_{10}$ capsules that were then welded shut and placed into the water-pressurized autoclave. Capsules were loaded with as many/as much of the samples while still allowing for the capsule to be cleanly welded shut without damage to the sample. Samples were cut into pieces in order to load into capsules. The weights of the capsules were taken prior to and after the experiment to determine if water infiltrated the capsule due to a failed weld (see Online Supplemental material).

Some fresh feathers (white and dark) were highly matured at 250°C/250 bars for 24 hours which resulted in a thick fluid (Saitta et al. 2017). The remaining samples (Table 1) moderately matured in this study were heated to 100°C/250 bars for 24 hours to allow for maturation while still maintaining enough morphological structure for microscopic analysis.

Structural Analysis

Structure was analyzed using light microscopy and SEM on portions of the matured and non-matured samples listed in Table 1.

Fresh samples were dehydrated prior to microscopy (decayed and matured samples were not). Samples were fixed in 10% neutral buffer formalin for 24 hours then dehydrated using an ethanol series according to standard histological protocol (Bancroft and Gamble 2002). Samples were then air dried using hexamethyldisilazane (HMDS) in a fume hood.

Decayed feathers underwent three different treatments in preparation for microscopy. For each feather type, some of the sample either had (1) no treatment prior to gold-coating; (2) dehydration using HMDS; or (3) 2% Triton X-100 detergent wash (30 minutes) followed by dehydration. Dehydration using HMDS alone was done in the hopes of preserving the microbial community on the feathers while the Triton X-100 wash was intended to remove the microbial community to allow for clear study of the feather.

Samples were then mounted on aluminum stubs using double-sided carbon tape and imaged using a Leica M205 C stereomicroscope with a Leica DFC425 C camera. Some larger samples had to be cut in order to fit well onto the stub (e.g., feathers) and others were cut in order to view them in cross section (e.g., feather rachises, turkey bristles, horse hair, and scales). Mounted stubs were sputter coated with gold and imaged using a Hitachi S3500N variable-pressure (environmental) scanning electron microscope.

The highly matured feather fluid samples were also observed in SEM by cutting open the capsule used during the maturation experiment and allowing the fluid to extrude out onto the surface of the capsule. The capsule was then affixed to SEM stubs using double-sided carbon tape. These samples were not dehydrated, nor were they gold coated as the Au^{90} Pd^{10} capsule onto which the thick fluid extruded provided enough charge dissipation.

Degradation extent was described qualitatively for each sample relative to other comparable samples or different treatments on that sample type.

RESULTS

Fresh Samples

The various integumentary structures show typical morphologies and ultrastructures as have been described in the literature (e.g., Schorger 1957; Lucas and Stettenheim 1972; Wyld and Brush 1983; Hill et al. 2010). However, certain observations were of particular interest.

Turkey bristles tended to fray or split when cut for cross-section examination, unlike feathers and hair. Unlike feathers, bristles were often solid in cross-section, especially in the juvenile beard, but had a more organized internal keratin structure than the mammalian hair. Flaking of the outer keratin ultrastructural surface was seen in bristles and hair. The cross sections of bristles from the juvenile turkey were more irregular than those of the adult, and some of the adult bristles had hollow centers.

As expected, feather barbules showed great variation in morphology and barbules in the iridescent portion of the turkey feathers showed a unique, broadened morphology. Some feather rachises cross-sections lacked a columnar organization of the keratin in the outer cortex.

The crocodile scales had a rippled ultrastructural surface of their outer layer and the avian reticulate scales also had a rough ultrastructural surface, while the avian scutate scale has a relatively smooth ultrastructural surface.

Decayed Samples

The control feathers showed no major signs of degradation, even at the ultrastructural level.

The decayed black feathers showed the highest level of degradation resulting in a ‘lint-like’ mass (Fig. 1A). The remnants were mostly dark (pieces of interlocking and partially fused barbs and barbules) with a few white remnants of the calamus or rachis. The ultrastructural surface of barbs and barbules was in the process of flaking and the surface of the rachis or calamus showed a degraded, woven texture (see Online Supplemental material). Exposed eumelanosomes were apparent with a microbial explanation ruled out as these structures were observed on the sample washed with Triton X-100. The broth in which the feathers were treated was darkened.

The decayed iridescent feathers had the second highest level of degradation resulting in a mass of slightly larger pieces of feather than in the decayed black feather. Slightly more morphological structure remained, but as in the decayed black feather, much of the mass consisted of barbs and barbules with a few rachis remnants. Iridescence was preserved in some of the barbs. The keratin showed a wrinkled, frayed, flaked, or woven ultrastructural surface.

Exposed medulloid cells from the pith (some of which are imploded) and potential melanosomes were apparent. The broth in which the feathers were treated was darkened.

The decayed white feathers (Fig. 1B) were the least noticeably degraded, with full feather morphology preserved, resembling the condition of the control feathers. There was some ultrastructural degradation with flaking on a calamus and one region on a rachis with small hair-like structures extending off the surface. The broth in which the feathers were treated remained relatively clear.

Matured Samples

Bristles.—The moderately matured adult turkey beard showed wrinkled and flaking bristle ultrastructural surfaces in various regions with compressed cross-sections common. The associated epidermis was degraded and flaking at the ultrastructural level.

The moderately matured juvenile turkey beard (Fig. 2F) showed curled, roughened bristles compared to the fresh sample (Fig. 2E) and discolored, flaking epidermis at the ultrastructural level. Bristle cross sections were compressed but the internal keratin still was organized.

Non-Decayed Feathers.—Moderately matured black feathers lacked overall feather morphology (e.g., Fig. 2C) but remnants showed the original range of coloration. Barbs and barbules were curled and kinked (Fig. 2D) but rachises could not be located.

Moderately matured iridescent feathers showed clumped, folded barbs with some iridescence remaining. Barb morphology was well preserved despite many of the barbs and barbules being incomplete with wrinkled ultrastructural surfaces. Part of the rachis was present and flaking on its ultrastructural surface.

Moderately matured white feathers mostly preserved the rachis/calamus whose ultrastructural surface was wrinkled, cracked, flaked, and frayed into strips along with some plumulaceous barbs with wrinkled and flaked ultrastructural surfaces present.

Decayed Feathers.—Moderately matured decayed black feathers became a black pellet of fused barbs and barbules with some flat, cracked or granulated regions derived from the rachis. Although some barbules were attached to barbs and had flattened with degraded surfaces, most of the feather structure was lost.

Moderately matured decayed iridescent feathers may have been exposed to water through a failed capsule seal during maturation, although the results are similar to other experimentally treated feathers, suggesting that such exposure likely had minimal effect. A black pellet was produced with the rachis remnant surface cracked and frayed into strands/strips that had irregular cross-sectional shape, were folded and creased, and were sometimes associated with thin filaments. Shriveled barbules were attached to barb remnants.

The moderately matured decayed white feather mostly preserved the rachis/calamus and had the highest level of ultrastructural degradation of any feather sample besides those that were highly matured. One end of the sample showed plumulaceous barbs. The calamus surface was woven-textured and cracked in some regions. The basal portion of the calamus showed internal layering of well-organized, overlapping strands with regularly spaced nodes that originated from the less degraded region of the calamus and are almost identical in appearance to plumulaceous barbules (Fig. 1C).

Hair.—Moderately matured hair was curled and extremely kinked, sometimes occurring in a helical pattern (Fig. 2A, 2B), with flaking on the ultrastructural surface and some split strands. The cross-section was solid but disorganized.

Scales.—The moderately matured predominantly black crocodile scale retained some color patterning, sublayers of the outer layer (epidermis) were splitting apart, and the rippled ultrastructure on the outer surface was retained (Fig. 3A, 3B). The internal layer (dermis) became pliable and degraded.

The moderately matured predominantly white crocodile scale consisted of brittle and pliable remnants deriving from the epidermis and dermis of the scale, respectively. Light coloration was preserved despite some discoloration of the epidermal surface. Cracking, flaking and splitting between sublayers was seen at the ultrastructural level in the corneous epidermis, with rippled ultrastructural surfaces preserved. The dermis is pitted and degraded.

Avian reticulate scales respond heterogeneously to moderate maturation with the corneous epidermis of the scale showing a brittle texture (with flaked ultrastructural surface and original sublayers preserved with wrinkled surface) and the dermis displaying a pliable texture. In general, moderately matured avian reticulate scales were more pliable than the fresh sample.

The moderately matured avian scutate scale became more pliable than the fresh sample (Fig. 3C) with presumably relatively more brittle and pliable regions deriving from corneous epidermis and dermis, respectively. The ultrastructural surface of the epidermis was wrinkled and flaked with a rough texture apparent in some areas (Fig. 3D).

Highly Matured Feathers.—Both dark and white highly matured feathers became a brownish, thick fluid with no ultrastructural features, such as melanosomes, visible.

DISCUSSION

Fresh Samples

Although the morphology and ultrastructure of these samples matched that expected from the literature, some observations are potentially novel. Unlike feathers and hair, turkey bristles tended to fray or split when cut. This may be due to their unique keratin type, which is a combination of feather and avian scale-type ϕ-keratin. It may also be due to the internal structure of bristles, which consists of irregularly shaped cross-sections that, unlike feathers, are sometimes solid, especially in immature bristles. Unlike hair, the internal structure of bristles contains organized internal keratin. Bristle ultrastructural surface flaking was more similar to α-keratin hair than to ϕ-keratin feathers. Ontogenetic changes observed here are consistent with those previously reported (Schorger 1957)—juvenile bristles are more irregular in cross-sectional shape and were not observed to show hollow centers, unlike some of the adult bristles.

Cross-sectional morphology is indeed highly varied among integumentary appendages, likely representing differences in development. Although it has been suggested that many fossil filaments in non-avian dinosaurs were hollow based on dark banding patterns (Chen et al. 1998; Mayr et al. 2002), the rationale behind these claims have been contradictory. Dark banding on the edges of the filament or in the center of the filament have both been described as evidence for a hollow structure. Evidence for such claims is also unconvincing. Dark banding usually represents melanin pigmentation and may not provide much information about internal structure. This was clarified by laser stimulated fluorescence (LSF), revealing a morphology consistent with an internal pith in the filaments of *Psittacosaurus* (Mayr et al. 2016) preserved via phosphate residues. More attempts with appropriate techniques (e.g., LSF) should be made to examine internal morphology of fossil integumentary structures given the potential developmental information that could be revealed.

The variation in barbule morphology observed among the feather samples is expected, even with regards to a unique broadened morphology associated with iridescent feather regions. A more peculiar result is that some rachises appeared to lack the columnar cross-sectional keratin

organization in their outer cortex. Whether or not this is genuine (potentially a result of amorphous keratin obscuring more organized keratin structure) should be investigated in the future as such a morphology might impact feather biomechanics.

Decayed Samples

Melanized feathers underwent more extensive decay compared to non-melanized feathers. White feathers appeared largely unaffected during the treatment although ultrastructural hair-like projections on the surface may represent early decay. This pattern was contrary to previous reports (Gunderson et al. 2008) that suggested that melanin slowed microbial decay rates. Recent studies have also highlighted the preferential colonization of bacteria to non-melanized parts of feathers (Justyn et al. 2017). This discrepancy might be a result of inconsistency in the inoculating microbes' ability to grow or multiply on the different feather samples, meaning more controlled monitoring of the cultures would be necessary. However, it is plausible that other feather characteristics might play a larger role in decay rate than melanin such as feather structure, calcium phosphate concentration, or the nature of surface lipids as these likely varied among the samples tested. Better-controlled feather decay experiments should be performed in the future to disentangle such variables.

It should be noted that surviving components of the decayed black feathers were mostly highly melanized barb regions and not the less melanized distal ends of the barbs or the rachis. However, the more uniformly melanized decayed iridescent feathers also showed preferential degradation of the rachis, suggesting that decay patterns are related to feather structure.

It appears that the connection between barbules and barbs is more easily preserved than those between the barbs and rachis in these decayed melanized feathers. The decayed black and iridescent feathers showed degraded woven textures to their keratin surfaces, and fraying was also observed in the decayed iridescent feathers. These textures likely represent early stages of keratin degradation. Keratin decay subsequently revealed eumelanosomes and medulloid cells.

The darkening of the broth used to treat the decayed black and iridescent feathers, unlike the relatively clear broth of the white feathers, might indicate that melanosomes/melanin were being lost from the keratin and leaching into the solution during decay.

Matured Samples

Moderate maturation dramatically altered morphology and ultrastructure of the keratinous appendages across all of the samples. Different keratin types and integumentary structures appeared to show different degradation patterns as a result of moderate maturation.

Bristles.—Although both adult and juvenile moderately matured turkey bristles had degraded surfaces and cross-sectional compression, the juvenile bristles were curled while the adult bristles were wrinkled or creased. Such differences could be due to the dried nature of the adult samples and/or the fact that adult bristles are more likely to have hollow centers.

Non-Matured Decayed Versus Moderately Matured Feathers.—Moderately matured black feather remnants retained black and white color range better than non-matured decayed black feathers. Both resulted in a mass of barbs and barbules, but unlike the decayed sample, no semi-fusion of these was observed in the moderately matured sample. These moderately matured barb and barbule remnants also showed kinking rather than surface degradation as in the decayed sample.

Both moderately matured and non-matured decayed iridescent feathers consisted of a mass of barbs and barbules and retained some degree of iridescence (although more reduced in the moderately matured sample). Similar to the observations of black feathers, moderately

matured iridescent feathers showed a loss of overall feather morphology while their keratin surface was less degraded than that of non-matured decayed iridescent feathers.

Such differences between moderately matured and decayed samples likely result from differences in degradation patterns produced by maturation versus microbial decay. Microbial decay has received much attention in experimental taphonomy for its unique roles in fossilization, such as inducing authigenic mineralization (e.g., Briggs 2003).

Non-Matured Decayed Versus Moderately Matured Decayed Feathers.—The moderately matured decayed black feathers had more extensive fusion of barbs and barbules than did the non-matured decayed black feathers. Keratin ultrastructural surface flaking of the non-matured decayed sample was intensified into a granulated texture in some regions of the moderately matured decayed sample.

Moderately matured decayed iridescent feathers resulted in a pellet (similar to moderately matured decayed black feathers). Although barbules attached to barbs are still present, more structure was lost in the moderately matured decayed sample than in the non-matured decayed sample. While the non-matured decay sample shows a woven keratin texture, keratin potentially derived from the rachis of moderately matured decayed sample was peeling into strips.

Maturation intensifies degradation initiated by microbial decay.

Unique Results from White Feathers.—Moderately matured white feathers showed a loss of overall feather morphology. Rachis/calamus keratin peeled into strips. Non-matured decayed white feathers showed hardly any degradation. The most extreme degradation texture results from a combination of decay and moderate maturation. An organized mesh of filaments is consistent with those reported from a microbial decay experiment on feathers (Lingham-Soliar et al. 2010). Filaments here appeared almost identical to plumulaceous barbules as did those previously reported, suggesting that these filaments are more recalcitrant than the surrounding amorphous keratin in which they reside. This similarity was argued by Lingham-Soliar et al. (2010) to represent evidence that the rachis evolved from the fusion of barbules. Although this study supports the existence of these rachis subunits, it is interesting that they were only observed after decay and moderate maturation, rather than decay alone as reported by Lingham-Soliar et al. (2010). The woven texture seen in some non-matured decayed feathers and peeling into strips seen in some moderately matured and moderately matured decayed feathers might represent earlier stages of keratin degradation whereby exposure of the filamentous subunits is a more extreme stage. Decay appears to result in a woven keratin surface in feathers, while moderate maturation produces peeling.

Decay Versus Maturation.—Unlike decay, moderate maturation resulted in more dramatic degradation (morphological and ultrastructural) in non-melanized, compared to melanized, feathers. This suggests that melanin might reduce the rate of feather degradation during maturation.

Among the experimental feathers, microbial decay acted upon the keratin surface to produce ultrastructural degradation textures while maturation tended to act upon the structure as a whole to distort filament shape rather than just its surface. Both could result in loss of overall feather morphology. Such differences are not unexpected given that bacteria and fungi are known to secrete metalloenzymes and keratinases onto the surface of keratin (Gupta and Ramnani 2006), meaning that microbial decay should primarily affect the surface of the keratin. The greatest degradation occurred in moderately matured decayed feathers. It must be kept in mind, that with regards to taphonomy, an organism or integumentary structure will likely first be

exposed to microbial decay (on the surface and in the sediment) long before it is buried deep enough for maturation.

Filament Distortion via Moderate Maturation.—Among filamentous structures (i.e., feathers, hair, and bristles), differences in moderate maturation patterns may relate to keratin type: hair (α-keratin) helically curled and kinked, juvenile turkey bristles curled while adult bristles wrinkled and creased (feather-type and avian scutate scale-type ϕ-keratin, keeping in mind the dried nature of the adult bristles), and feather barbules kinked (feather-type ϕ-keratin). If such distortions of filament shape were recorded in the remaining melanosome or calcium phosphate positioning (or as an impression in the surrounding matrix) after keratin was lost, such information could survive into the fossil record. However, it seems unlikely that such maturation would occur prior to significant keratin protein loss from microbial decay, and even if microbial decay were to be limited by conditions such as anoxia, then chemical degradation and loss of the keratin protein via reactions like hydrolysis might precede thermally-induced filament distortions during diagenesis. It is also uncertain whether such filament distortions would occur when tightly surrounded in a sediment matrix during diagenesis.

Scales.—Both predominantly black and white moderately matured crocodile scales had a cracked outer layer, splitting between sublayers of the outer layer, and retention of rippled ultrastructural texture. The predominantly white sample was slightly discolored and the predominantly black sample retained the original color range. Internal scale layers became pliable.

Moderately matured avian reticulate scales also had brittle and pliable remnants like the moderately matured crocodile scales (see detailed discussion of degraded dermis in following section).

The moderately matured avian scutate scale had brittle and pliable portions as did other moderately matured scales. However, those in the moderately matured avian scutate scale were more difficult to distinguish than in the other moderately matured scale samples and had less ultrastructural features. Therefore, brittle and pliable remnants of scales deriving from outer corneous and inner dermis layers, respectively, after moderate maturation were more recognizable in non-featherlike β-keratin scales than avian scale-type ϕ-keratin.

Rippled ultrastructural surfaces on the outer layer of fresh and moderately matured crocodile and fresh avian reticulate scales (both of which are non-featherlike β-keratin) were not seen on the surfaces of feathers or avian scutate scales (both of which have smooth surfaces and are ϕ-keratin). If ultrastructure is an accurate indicator of keratin type, and the rippled texture survives moderate maturation, it does not necessarily mean that it can survive higher maturation during diagenesis or that the keratin texture can survive microbial decay or chemical degradation via reactions like hydrolysis prior to deep burial. It is uncertain whether or not a mineral matrix could produce a mold of such ultrastructural textures that would persist or be detectable in the fossil record. Sediment-based maturation experiments would be required to test this, and no fossils have yet been reported with this texture preserved. Similar ultrastructure might provide further evidence that avian scutate scales derived from feathers (Zheng et al. 2013).

Self-Organizing Structures and Taphonomic Artifacts in Keratin.—The dermis of the moderately matured avian reticulate scales displays many pits, folds, and bulges (Fig. 4A). The extreme morphology, a concave bulge, superficially resembles the appearance of mammalian erythrocytes. Many intermediate structures were produced between the extreme morphology and simple folding or pitting. Some bulges are irregularly shaped or spherical. These structures likely represent taphonomic artifacts where degraded organic material becomes pliable and folds

outward (or gasses escape from the interior) during moderate maturation or evacuation of the sample chamber for SEM.

Very similar organic features interpreted by Bertazzo et al. (2015) as fossil erythrocytes (with internal structures interpreted as nuclei) in Mesozoic dinosaur bones (Fig. 4B) also vary morphologically. Most are folds protruding from and connected to a continuous organic material similar to the extreme morphology observed in the scales, although simpler, smaller pits and bulges are present. Proposed nuclei revealed through focused ion beam sectioning are likely just pockets of varying density within folds. Supplementary material of Bertazzo et al. (2015, movie 1) suggests that each 'erythrocyte-like' structure contains several of these dense areas, contradicting their identification as nuclei. These proposed erythrocytes show more superficial similarity in shape to mammalian erythrocytes than to those of birds or crocodilians, which are oval rather than circular (Claver and Quaglia 2009). Bertazzo et al. (2015) described the structures as ~ 2 μm in diameter. Bird erythrocytes are ~ 4.5–7.5 times larger. The largest structures observed in our experiments are an order of magnitude larger (~ 20 μm). However, our experimental sample shows a range of morphologies and sizes—the smallest being pits or blebs ~ 1–2 μm in diameter.

Variation in the structures' size, either within a sample or between the scales and the dinosaur fossil, is potentially a result of differing viscosity of the organic material, affecting folding periodicity and, therefore, size. Differing pliability of the original organic material might explain differing viscosity of the degraded material. Our structures were produced from dermal tissue while structures in the fossil might derive from relatively recent biofilms infiltrating the bone rather than recalcitrant endogenous molecules (e.g., lipids from cell walls, which may not preserve original cell morphology). Variation in diagenetic (fossil) or maturation (scales) conditions might affect the material's pliability or structures' size. If diagenesis/maturation alone cannot produce the folds, maybe diagenesis/maturation produces degraded organics that are shaped through vacuum during SEM/sample coating via gas escape. The degree to which the chamber is evacuated might affect the size of the structures.

Shared 'erythrocyte-like' morphology and organic nature of the experimental and fossil structures suggests correlation. The variation exhibited is consistent with abiotic formation. Self-organizing structures (SOS) can form abiotically and are characterized not by a lack of complexity compared to biotic structures, but by a wider range of morphologies (Brasier et al. 2006). The structures in the fossil and scales vary from ~ 2–20 μm, while bird erythrocytes vary interspecifically from 9–15 μm in diameter (Sturkie 1986; Gregory 2001). The size and morphology ranges suggest that they are SOS formed from abiotic taphonomic processes on degraded organic material. Disparate tissues (i.e., dermis vs. unknown organics in the fossil) can produce the similar ultrastructures, suggesting that they are a common product of physical alteration of degraded organics rather than unique endogenous bone tissue. Given the open system dynamics of bone, the degraded organics in the fossils may be relatively recent microbial contamination (the fossils were museum specimens that had not been sterilely collected or stored).

Other proposed 'intravascular microstructures' have wide size ranges (Pawlicki and Nowogrodzka-Zagórska 1998; Schweitzer et al. 2007; Schweitzer 2010) (Fig. 4C; also see "Early Discovery" panel in Schweitzer 2010, p. 64). The requirement that the same taphonomic conditions would lead one of two adjacent erythrocytes to shrink, but not the other, raises doubts that they represent endogenous cells. Such previously described structures compositionally differ

from the organic folds of Bertazzo et al. (2015) and have been alternatively described as iron oxide or pyrite framboids (Martill and Unwin 1997; Kaye et al. 2008).

Erythrocytes in human bone are histologically unidentifiable after a week, indicating rapid cell morphology loss. Erythrocyte breakdown products are undetectable immunohistochemically more than a few years post-mortem or in archaeological bones (Capella et al. 2015), suggesting protein breakdown and antigen binding site loss. Rapid decay in archaeological settings bodes poorly for Mesozoic erythrocytes persisting through diagenesis.

Time of flight secondary ion mass spectrometry (TOF-SIMS) of a blood-engorged mosquito found in middle Eocene oil shales (Greenwalt et al. 2013) detected highly stable porphyrins (Falk and Wolkenstein 2017) derived from the heme cofactor of haemoglobin, although the protein and phospholipids had decomposed. In contrast, Bertazzo et al. (2015) used energy dispersive X-ray spectroscopy to reveal that their structures are carbon-enriched, neither specifying their precise nature nor proving endogenecity. Similar TOF-SIMS spectra to fresh emu blood likely only verifies the organic nature of these structures. Quantitative analysis of the spectra, e.g., through principal component analysis, using further organic controls, e.g., humic acids or biofilms, is needed to demonstrate similar chemistries between the structures and emu blood since the partial least square-discriminant analysis by Bertazzo et al. (2015) lacks such controls. Putative folic acid and lipid peaks could easily come from bacteria.

Highly Matured Feathers.—Detailed discussion of the chemical composition of highly matured feather samples are reported in Saitta et al. (2017). Structurally, these samples completely degraded to become a thick fluid. Melanosomes were not visible when examining the surface of the fluid but could have been present and not visible within the fluid, but such an investigation was not carried out due to time and resource constraints. Isolated melanosomes are known to survive these autoclave conditions (Colleary et al. 2015). The complete loss of structural information in these samples is worrying as it suggests that such information like texture will be lost in fossils that undergo full diagenesis.

Only calcium phosphate or pigmentation (e.g., melanin/melanosomes) of the integumentary structure can persist in the fossil record and reports of keratin's ability to persist in fossils and through diagenesis likely represent false positives (Saitta et al. 2017). An excellent example of a fossil whose integumentary structures are preserved as phosphates and melanin is the exceptional *Psittacosaurus* specimen, SMF R 4970 (Mayr et al. 2016; Vinther et al. 2016). At the moment, it is in unclear whether filament distortion could be recorded in calcium phosphate or melanosome position or if scales with ultrastructural ripples can result in a mineral mold on the adjacent matrix to preserve such a texture.

CONCLUSION

The results of this study suggest that melanization may not be the main factor in conferring decay resistance to feathers but may play a role in retarding feather degradation as a result of maturation. We also find further support for the existence of rachis subunits very similar in appearance to plumulaceous barbules. Structures produced through maturation suggest that dinosaur 'erythrocytes' (Bertazzo et al. 2015) are degraded organics folded via diagenesis or SEM/sample coating vacuum, not cells. Given the open-system of bones (Bada et al. 1999), extreme amount of time this system has been allowed to flux, and geologic instability of nucleic acids, phospholipids, and proteins (Briggs and Summons 2014), they may not be endogenous organics, but instead microbial contamination.

The ability to distinguish keratin types based upon distortion of integumentary filaments or the survivability of keratin-specific ultrastructural textures in scales during moderate

maturation could lead some to conclude that an indication of the original chemistry of an integumentary appendage might persist in the fossil record. Given the low fossilization potential of proteins, the only possible avenues for these patterns to fossilize are in the components of keratinous structures known to persist over geologic time, such as calcium phosphate or pigmentation (e.g., Mayr et al. 2016), or in a mold produced by the adjacent matrix (if it is even possible for such fine ultrastructural details to produce a mold). However, none of these textures have been observed or reported in fossils and three main problems are made apparent with regards to recovering such information. First, the effect of the sediment and environment during diagenesis was not tested here, so whether, for example, filaments matured within a sediment matrix will show the same distortions is questionable (Briggs and Williams 1981). Second, microbial decay or chemical degradation is expected to occur much earlier in taphonomy than maturation as it takes a long time for an organism or integumentary appendage to be buried to diagenetic depth. Thus, any differences in maturation between keratin types might be a moot point if the keratin decays prior to diagenesis. This is likely the case for many keratinous fossils given the prevalence of specimens with shrunken melanosomes residing inside sediment molds, indicating keratin decay and subsequent sediment infilling prior to diagenetic maturation significant enough to alter the melanosomes. And third, highly matured feather samples show complete structural breakdown, suggesting that even if keratin were to survive long enough to be deeply buried, the most extreme diagenetic conditions will likely destroy all structural information with regards to textural features that might provide information about the keratin protein itself. Thus, much of the taphonomic patterns observed here are potentially more applicable to the archaeological (e.g., when examining corrosion casts) rather than paleontological record, unless it can be shown that such textures or distortions are recognizable in either the surviving, non-protein components of keratinous tissues or in impressions such tissues leave behind in the adjacent matrix. For example, given amber's ability to preserve fine, three-dimensional morphological details, such an environment may warrant investigation for these textures whose preservation would likely be a function of the rate of keratin degradation relative to the rate of resin hardening and polymerization.

ACKNOWLEDGMENTS

Many thanks to Antoine Soler (La Ferme aux Crocodiles) for dissecting and shipping the crocodile skin, Stuart Kearns and Ben Buse for assistance with the SEM, and T.A. Dececchi and an anonymous reviewer of the manuscript.

SUPPLEMENTAL MATERIAL

Data are available from the PALAIOS Data Archive:
http://www.sepm.org/pages.aspx?pageid=332.

REFERENCES

Alibardi, L., Knapp, L.W., and Sawyer, R.H., 2005, Beta-keratin localization in developing alligator scales and feathers in relation to the development and evolution of feathers: Journal of Submicroscopic Cytology and Pathology, v. 38, p. 175–192.

Bada, J.L., Wang, X.S., and Hamilton, H., 1999, Preservation of key biomolecules in the fossil record: current knowledge and future challenges: Philosophical Transactions of the Royal Society of London B: Biological Sciences, v. 354, p. 77–87.

Bancroft, J.D. and Gamble, M., 2002, Theory and Practice of Histopathological Techniques: Churchill Livingstone, New York, 744 p.

Bertazzo, S., Maidment, S.C., Kallepitis, C., Fearn, S., Stevens, M.M., and Xie, H.N., 2015, Fibres and cellular structures preserved in 75-million-year-old dinosaur specimens: Nature Communications, v. 6, 7352. doi: 10.1038/ncomms8352.

Brasier, M., McLoughlin, N., Green, O., and Wacey, D., 2006, A fresh look at the fossil evidence for early Archaean cellular life: Philosophical Transactions of the Royal Society of London B: Biological Sciences, v. 361, p. 887–902.

Briggs, D.E.G., 2003, The role of decay and mineralization in the preservation of soft-bodied fossils: Annual Review of Earth and Planetary Sciences, v. 31, p. 275–301.

Briggs, D.E.G. and Summons, R. E., 2014, Ancient biomolecules: their origins, fossilization, and role in revealing the history of life: BioEssays, v. 36, p. 482–490.

Briggs, D.E.G. and Williams, S. H., 1981, The restoration of flattened fossils: Lethaia, v. 14, p.157–164.

Brom, T.G., 1986, Microscopic identification of feathers and feather: Bijdragen tot de dierkunde, v. 56, p. 181–204.

Brush, A.H., 1978, Feather keratins: Chemical Zoology, v. 10, p. 117–139.

Cappella, A., Bertoglio, B., Castoldi, E., Maderna, E., Giancamillo, A.D., Domeneghini, C., Andreola, S., and Cattaneo, C., 2015, The taphonomy of blood components in decomposing bone and its relevance to physical anthropology: American Journal of Physical Anthropology, v. 158, p. 636–645. doi: 10.1002/ajpa.22830.

Chen, P.J., Dong, Z.M., and Zhen, S.N., 1998, An exceptionally well-preserved theropod dinosaur from the Yixian Formation of China: Nature, v. 391, p. 147–152.

Claver, J.A. and Quaglia, A.I., 2009, Comparative morphology, development, and function of blood cells in nonmammalian vertebrates: Journal of Exotic Pet Medicine, v. 18, p. 87–97.

Colleary, C., Dolocan, A., Gardner, J., Singh, S., Wuttke, M., Rabenstein, R., Habersetzer, J., Schaal, S., Feseha, M., Clemens, M., and Jacobs, B.F., 2015, Chemical, experimental, and morphological evidence for diagenetically altered melanin in exceptionally preserved fossils: Proceedings of the National Academy of Sciences, v. 112, p. 12592–12597.

Dove, C.J., Hare, P.G., and Heacker, M., 2005, Identification of ancient feather fragments found in melting alpine ice patches in southern Yukon: Arctic, v. 58, p. 38–43.

Falk, H. and Wolkenstein, K., 2017, Natural product molecular fossils, *in* A.D. Kinghorn, H. Falk, S. Gibbons, and J. Kobayashi (eds.), Progress in the Chemistry of Organic Natural Products 104: Springer, New York, p. 1–126.

Fraser, R.D.B., MacRae, T.P., and Rogers, G.E., 1972, Keratins—Their Composition, Structure and Biosynthesis: Charles C. Thomas, Springfield, Illinois, 304 p.

Godefroit, P., Sinitsa, S.M., Dhouailly, D., Bolotsky, Y.L., Sizov, A.V., McNamara, M.E., Benton, M.J., and Spagna, P., 2014, A Jurassic ornithischian dinosaur from Siberia with both feathers and scales: Science, v. 345, p. 451–455.

Greenwalt, D.E., Goreva, Y.S., Siljeström, S.M., Rose, T., and Harbach, R.E., 2013, Hemoglobin-derived porphyrins preserved in a middle Eocene blood-engorged mosquito: Proceedings of the National Academy of Sciences, v. 110, p. 18496–18500.

Greenwold, M.J. and Sawyer, R.H., 2010, Genomic organization and molecular phylogenies of the beta (β) keratin multigene family in the chicken (*Gallus gallus*) and zebra finch (*Taeniopygia guttata*): implications for feather evolution: BMC Evolutionary Biology, v. 10, p. 148.

Greenwold, M.J. and Sawyer, R.H., 2011, Linking the molecular evolution of avian beta (β)

keratins to the evolution of feathers: Journal of Experimental Zoology Part B: Molecular and Developmental Evolution, v. 316, p. 609–616.
Gregory, T.R., 2001, The bigger the C-value, the larger the cell: genome size and red blood cell size in vertebrates: Blood Cells, Molecules, and Diseases, v. 27, p. 830–843.
Gunderson, A.R., Frame, A.M., Swaddle, J.P., and Forsyth, M.H., 2008, Resistance of melanized feathers to bacterial degradation: is it really so black and white?: Journal of Avian Biology, v. 39, p. 539–545.
Gupta, R. and Ramnani, P., 2006, Microbial keratinases and their prospective applications: an overview: Applied Microbiology and Biotechnology, v. 70, p. 21–33.
Hargrave, L.L., 1960, Identification of archeological feathers from Glen Canyon, Utah: University of Utah Anthropological Papers, v. 44, p. 239–241.
Hill, P., Brantley, H., and Van Dyke, M., 2010, Some properties of keratin biomaterials: kerateines: Biomaterials, v. 31, p. 585–593.
Justyn, N.M., Peteya, J.A., D'Alba, L., and Shawkey, M.D., 2017, Preferential attachment and colonization of the keratinolytic bacterium *Bacillus licheniformis* on black-and white-striped feathers: The Auk, v. 134, p. 466–473.
Kaye, T.G., Gaugler, G., and Sawlowicz, Z., 2008, Dinosaurian soft tissues interpreted as bacterial biofilms: PLoS One, v. 3, p. e2808.
Lingham-Soliar, T., Bonser, R.H., and Wesley-Smith, J., 2010, Selective biodegradation of keratin matrix in feather rachis reveals classic bioengineering: Proceedings of the Royal Society of London B: Biological Sciences, v. 277, p. 1161–1168.
Lucas, A.M. and Stettenheim, P.R., 1972, Avian Anatomy, Integument, Part 1, Agricultura Handbook 362: U.S. Department of Agriculture, Washington, D.C., 340 p.
Martill, D.M. and Unwin D.M., 1997, Small spheres in fossil bones: blood corpuscles or diagenetic products?: Palaeontology, v. 40, p. 619–624.
Mayr, G., Peters, S.D., Plodowski, G., and Vogel, O., 2002, Bristle-like integumentary structures at the tail of the horned dinosaur *Psittacosaurus*: Naturwissenschaften, v. 89, p. 361–365.
Mayr, G., Pittman, M., Saitta, E., Kaye, T.G., and Vinther, J., 2016, Structure and homology of *Psittacosaurus* tail bristles: Palaeontology, v. 59, p. 793–802. doi: 10.1111/pala.12257.
Messinger, N.G., 1965, Methods used for identification of feather remains from Wetherill Mesa: Memoirs of the Society for American Archaeology, v. 19, p. 206–215.
Moyer, A.E., Zheng, W., and Schweitzer, M.H., 2016, Keratin durability has implications for the fossil record: results from a 10 year feather degradation experiment: PloS one, v. 11, p. e0157699.
O'Connor, S., Solazzo, C., and Collins, M., 2015, Advances in identifying archaeological traces of horn and other keratinous hard tissues: Studies in Conservation, v. 60, p. 393–417.
Pan, Y., Zheng, W., Moyer, A.E., O'Connor, J.K., Wang, M., Zheng, X., Wang, X., Schroeter, E.R., Zhou, Z., and Schweitzer, M.H., 2016, Molecular evidence of keratin and melanosomes in feathers of the Early Cretaceous bird *Eoconfuciusornis*: Proceedings of the National Academy of Sciences, v. 113, p. E7900–E7907.
Pawlicki, R. and Nowogrodzka-Zagórska, M., 1998, Blood vessels and red blood cells preserved in dinosaur bones: Annals of Anatomy-Anatomischer Anzeiger, v. 180, p. 73–77.
Prum, R.O. and Brush, A.H., 2002, The evolutionary origin and diversification of feathers: The Quarterly Review of Biology, v. 77, p. 261–295.
Reinhard, K.J. and Bryant, V.M., 1992, Coprolite analysis: a biological perspective on archaeology: Archaeological Method and Theory, v. 4, p. 245–288.

Rogers, J.D., Dove, C.J., Heacker, M., and Graves, G.R., 2002, Identification of feathers in textiles from the Craig Mound at Spiro, Oklahoma: Southeastern Archaeology, v. 21, p. 245–251.
Saitta, E.T., Rogers, C.S., Brooker, R.A., Abbott, G.D., Kumar, S., O'Reilly, S., Donohoe, P., Dutta, S., Summons, R.E., and Vinther, J., 2017, Low fossilisation potential of keratin protein revealed by experimental taphonomy: Palaeontology, v. 60, p. 547–556.
Sawyer, R.H., Glenn, T., French, J.O., Mays, B., Shames, R.B., Barnes, G.L., Rhodes, W., and Ishikawa, Y., 2000, The expression of beta (β) keratins in the epidermal appendages of reptiles and birds: American Zoologist, v. 40, p. 530–539.
Sawyer, R.H., Washington, L.D., Salvatore, B.A., Glenn, T.C., and Knapp, L.W., 2003, Origin of Archosaurian integumentary appendages: the bristles of the wild turkey beard express feather-type β keratins: Journal of Experimental Zoology Part B: Molecular and Developmental Evolution, v. 297, p. 27–34.
Schorger, A.W., 1957, The beard of the wild turkey: The Auk, v. 74, p. 441–446.
Schweitzer, M.H., 2010, Blood from stone: Scientific American, v. 303, p. 62–69.
Schweitzer, M.H., Wittmeyer, J.L., and Horner, J.R., 2007, Soft tissue and cellular preservation in vertebrate skeletal elements from the Cretaceous to the present: Proceedings of the Royal Society of London B: Biological Sciences, v. 274, p. 183–197.
Solazzo, C., Rogers, P.W., Weber, L., Beaubien, H.F., Wilson, J., and Collins, M., 2014, Species identification by peptide mass fingerprinting (PMF) in fibre products preserved by association with copper-alloy artefacts: Journal of Archaeological Science, v. 49, p. 524–535.
Sturkie, P.D., 1986, Heart: contraction, conduction, and electrocardiography, *in* P.D. Sturkie (ed.), Avian Physiology: Springer, New York, p. 167–190.
Vinther, J., Nicholls, R., Lautenschlager, S., Pittman, M., Kaye, T.G., Rayfield, E., Mayr, G., and Cuthill, I.C., 2016, 3D camouflage in an ornithischian dinosaur: Current Biology, v. 26, p. 2456–2462.
Williams, C.M., Richter, C.S., Mackenzie, J.M., and Shih, J.C., 1990, Isolation, identification, and characterization of a feather-degrading bacterium: Applied and Environmental Microbiology, v. 56, p. 1509–1515.
Wyld, J.A. and Brush, A.H., 1979, The molecular heterogeneity and diversity of reptilian keratins: Journal of Molecular Evolution, v. 12, p. 331–347.
Wyld, J.A. and Brush, A.H., 1983, Keratin diversity in the reptilian epidermis: Journal of Experimental Zoology, v. 225, p. 387–396.
Xu, X. and Guo, Y., 2009, The origin and early evolution of feathers: insights from recent paleontological and neontological data: Vertebrata PalAsiatica, v. 47, p. 311–329.
Zhang, F., Zhou, Z., Xu, X., Wang, X., and Sullivan, C., 2008, A bizarre Jurassic maniraptoran from China with elongate ribbon-like feathers: Nature, v. 455, p. 1105–1108.
Zheng, X., Zhou, Z., Wang, X., Zhang, F., Zhang, X., Wang, Y., Wei, G., Wang, S., and Xu, X., 2013, Hind wings in basal birds and the evolution of leg feathers: Science, v. 339, p. 1309–1312.

FIGURE CAPTIONS

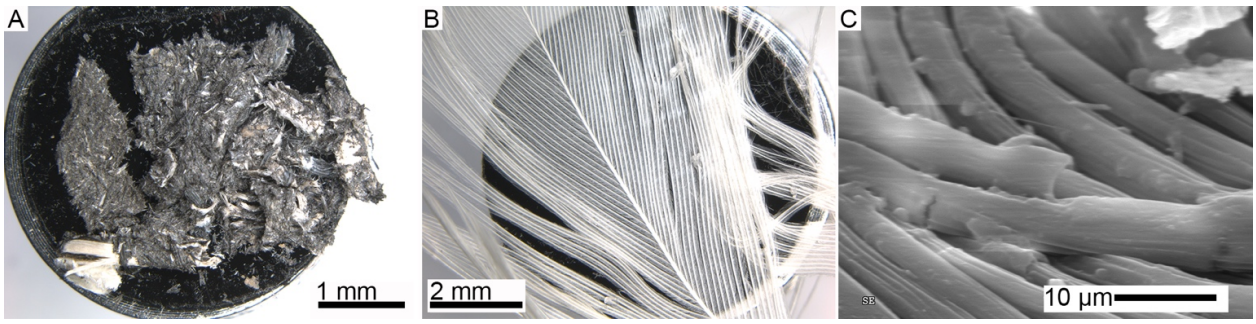

FIG. 1.—Variation in degraded feathers. **A**) Decayed black feathers on SEM stub. **B**) Decayed white feather on SEM stub. **C**) SEM image of decayed and moderately matured white feather revealing filamentous rachis subunits.

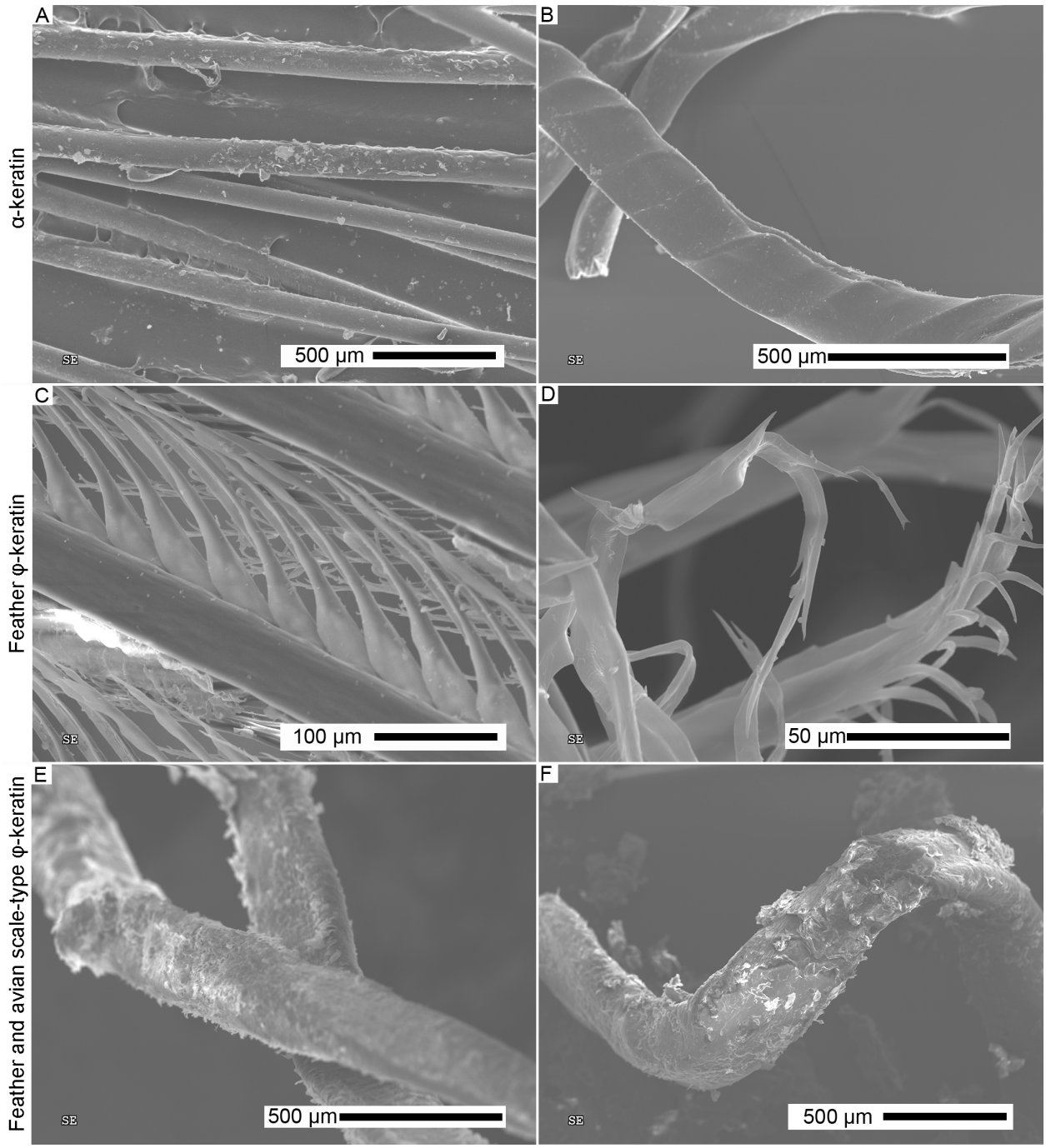

FIG. 2.—SEM images of keratinous filament ultrastructural deformation patterns under moderate maturation. **A**) Fresh horse hair. **B**) Moderately matured horse hair showing helical curling. **C**) Fresh black feather barbs and barbules. **D**) Moderately matured black feather barbules showing kinking. **E**) Fresh juvenile turkey beard bristles. **F**) Moderately matured juvenile turkey beard bristles showing curling.

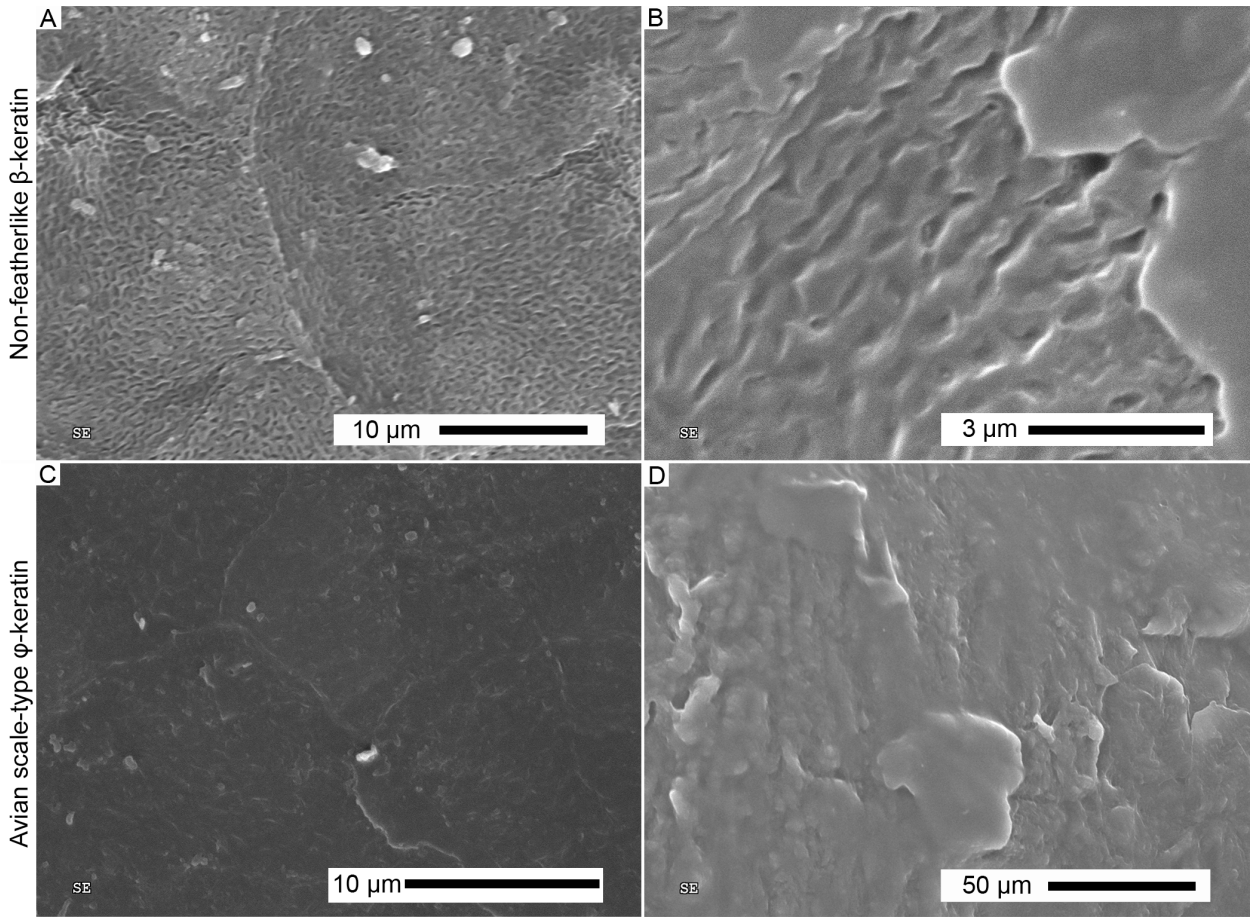

FIG. 3.—SEM images of ultrastructural variation and moderate maturation in scales. **A**) Fresh predominantly black crocodile scale with rippled ultrastructural surface. **B**) Moderately matured predominantly black crocodile scale with rippled ultrastructural surface preserved. **C**) Fresh avian scutate scale with smooth ultrastructural surface. **D**) Moderately matured avian scutate scale with degraded, but not rippled, ultrastructural surface.

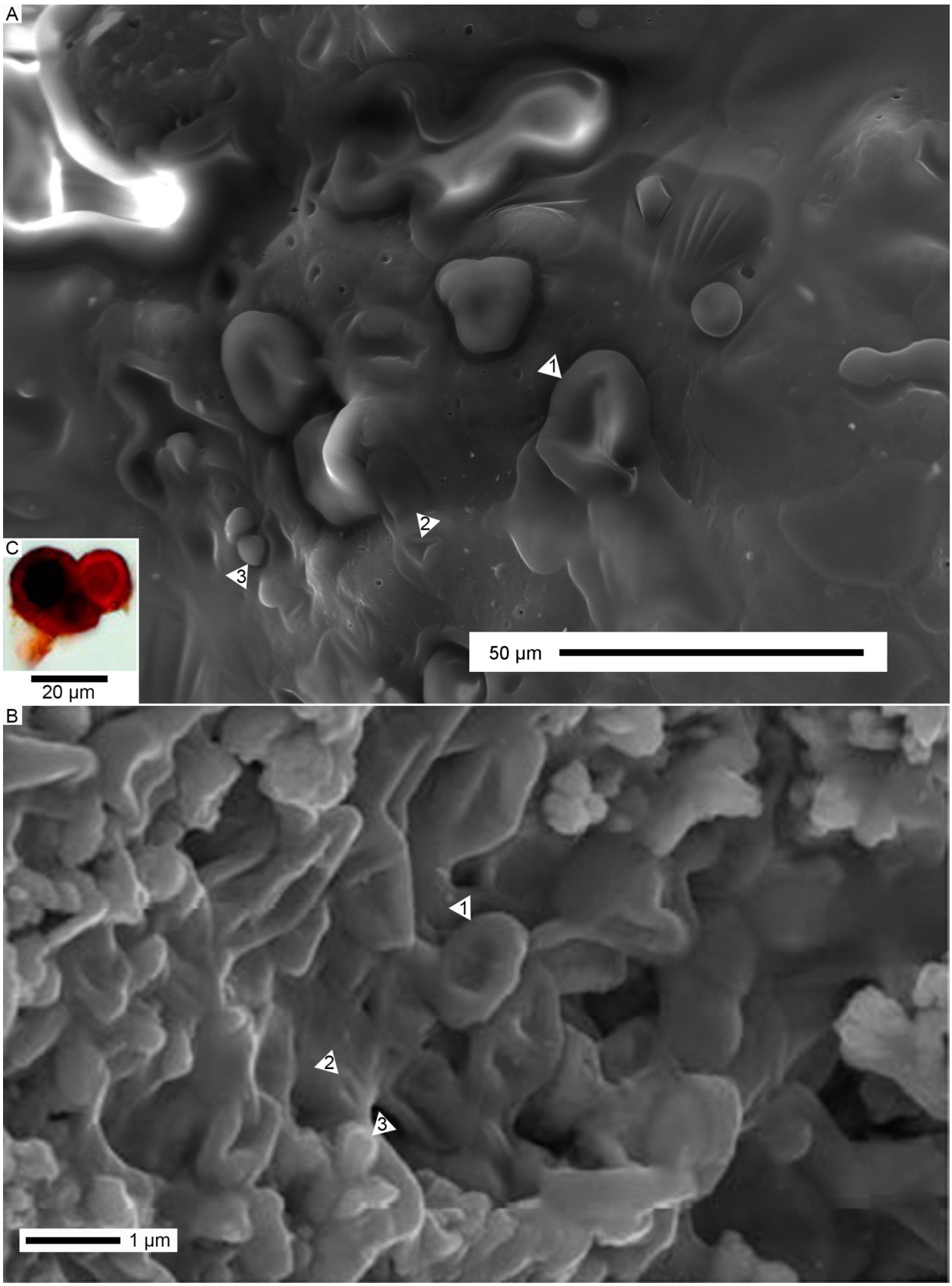
A
1
2
3
50 µm
C
20 µm
B
1
2
3
1 µm

FIG. 4.—Abiotically formed structures as an explanation for 'dinosaur blood'. **A**) Moderately matured avian reticulate scales. **B**) SEM image of proposed "erythrocyte-like structures" in a theropod ungual (NHMUK R4493) modified from Bertazzo et al. (2015, online Supplementary Fig. 3c) and used under Creative Commons CC-BY license. Presented here with a defined scale bar. Arrowheads indicate several shared morphologies: (1) extreme morphology of concave bulge/fold visibly continuous with the underlying organic material; (2) pit/simple fold; (3) spherical bulge. **C**) 'Intravascular microstructures' that have been identified as erythrocytes by some researchers (Schweitzer 2010). Image reproduced from Schweitzer et al. (2007, fig. 3p) with permission from The Royal Society.

TABLE CAPTION

Sample	Notes
Moderately matured - 100°C, 250 bars, 24 hours	
Feathers – iridescent	Turkey; Wing covert; Feather φ-keratin
Feathers – white	Chicken; Wing covert; Feather φ-keratin
Feathers – black	Chicken; Back/neck region; White fringe on vane; Feather φ-keratin
Avian scutate scales	Turkey; Avian scale-type φ-keratin
Avian reticulate scales	Turkey; Multiple scales with associated epidermis; Non-featherlike β-keratin
Turkey beard – adult	Dried samples; Small portion of epidermis still attached; Feather and avian scale-type φ-keratin
Turkey beard – juvenile	Portion of epidermis still attached; Feather avian scale-type φ-keratin
Crocodilian scale – black	Nile crocodile (*Crocodylus niloticus*); Flank region; Predominantly black coloration; Non-featherlike β-keratin
Crocodilian scale – white	Nile crocodile; Flank region; Predominantly white/light coloration; Non-featherlike β-keratin
Mammalian hair	Horse (*Equus ferus*) mane; Black color; α-keratin
Decayed feathers - iridescent	Turkey; Back region; Feather φ-keratin
Decayed feathers - white	Chicken; Back/neck region; Feather φ-keratin
Decayed feathers - black	Chicken; Back/neck (white fringe on vane) and tail regions; Feather φ-keratin
Highly matured - 250°C, 250 bars, 24 hours	
White feathers	Chicken (*Gallus gallus*); Leg region; Feather φ-keratin
Dark feathers	Turkey (*Meleagris gallopavo*); Leg region; Color gradient (from proximal to distal) of white, grey, black, and iridescent; Feather φ-keratin

TABLE 1.—List of samples and maturation runs. Samples that are not listed as decayed are fresh samples.